Iranian Journal of Analytical Chemistry
Volume 12, Spring 1, March 2025 (100-109) Original Research Article

مجله ایرانی شیمی تجزیه
دوره ۱۲، شماره ۱، فروردین۱۴۰۴ (۱۰۰-۱۰۹)

MnO_2 /MWCNTs Nanocomposite Modified Carbon Ceramic Electrode: A Renewable Platform for Ethanol Oxidation

Tahereh Rohani*[1], Sayed Zia Mohammadi[1], Masood Nayebli[1]

[1]Department of Chemistry, Payame Noor University, 19395-4697, Tehran, Iran

e-mail: Rohani@pnu.ac.ir

Received: 2 October 2024 **Accepted:** 22 October 2024
DOI: 10.30473/IJAC.2025.76680.1332

Abstract

In this study, a carbon ceramic electrode was fabricated and subsequently modified by manganese dioxide/multiwalled carbon nanotubes composite (MnO_2/MWCNTs). MWCNTs were hybridized with Manganese dioxide to enhance the electrocatalytic properties. The resulting nanocomposite was evaluated for its efficacy in catalyzing ethanol oxidation. Characterization of the catalyst was performed using X-ray diffraction (XRD), Scanning electron microscopy (SEM) and Fourier-transform infrared (FT-IR) spectroscopy. Electrochemical properties were studied using cyclic voltammetry (CV), differential pulse voltammetry (DPV) and chronoamperometry. The results indicate a linear range from 0.02 to 0.3 mM with a detection limit of 6.2 µM and a diffusion coefficient of $5.24 \times 10^{-7} cm^2 s^{-1}$ for ethanol. The high surface area and conductivity of MWCNTs, hybridized with the catalytic activity of MnO_2 , demonstrate the potential of the as-prepared nanocomposite for high performance fuel cell applications.

Keywords
Ethanol oxidation, Fuel cells, MnO_2 , Multiwalled carbon nanotubes

* Corresponding author:

T. Rohani; E-mail: Rohani@pnu.ac.ir

1. INTRODUCTION

As the global pursuit of clean and sustainable energy intensifies, fuel cell technology has emerged as a compelling alternative to traditional fossil fuels. Among the various fuel cell systems, direct ethanol fuel cells (DEFCs) have garnered significant attention for their ability to harness bioethanol, a renewable fuel derived from biomass such as sugarcane, corn, and cellulose [1,2]. Ethanol presents several notable advantages as a fuel source: it boasts a high energy density, is relatively easy to store and transport, and can be sustainably produced from agricultural feedstocks. Additionally, ethanol is less toxic than methanol, making it a safer option for widespread use. Despite these promising attributes, the advancement and commercialization of ethanol-powered fuel cells still face considerable challenges [3-6]. One of the primary challenges lies in achieving complete oxidation of ethanol to carbon dioxide, a process that requires the cleavage of carbon–carbon (C–C) bonds, an energetically demanding step. This often leads to the accumulation of partially oxidized byproducts such as acetic acid and acetaldehyde, which diminish the overall efficiency of the fuel cell. To address these limitations, researchers have focused on developing and optimizing catalytic materials capable of facilitating the full oxidation of ethanol, thereby enhancing the performance and viability of DEFCs [7,8]. Among these catalysts, carbon nanotubes (CNTs), due to their unique structure, high specific surface area, excellent electrical conductivity, and chemical stability, have attracted significant attention. However, previous studies have shown that carbon nanotubes alone exhibit limited catalytic activity in oxidation reactions [9-11]. So, to effectively utilize carbon nanotubes in catalytic reactions, surface modification with active compounds, particularly metal oxides, is essential [12,13]. In recent years, numerous carbon nanotube (CNT)/metal oxide heterostructures have been synthesized and extensively investigated for their electrochemical properties. For instance, Jiang et al. developed a highly sensitive nonenzymatic glucose sensor based on CuO nanoparticle-modified CNTs fabricated via sputtering deposition [14]. Similarly, Fang et al. reported a novel hydrazine sensor utilizing a CNT-wired ZnO nanoflower electrode, synthesized through an ammonia evaporation method [15]. Liu et al. also demonstrated the promising electrochemical performance of a CNT/Fe_3O_4 composite for glucose detection [16].

Among various metal oxides, manganese dioxide (MnO_2) is particularly promising for enhancing the catalytic performance of CNTs due to its strong oxidizing power, high catalytic activity, excellent chemical stability, low cost, and high energy density [17,18]. The combination of these two materials can lead to the development of hybrid catalysts with synergistic properties, offering superior efficiency in oxidation processes [19-22]. This study introduces a highly effective electrocatalyst designed for application in direct ethanol fuel cells (DEFCs) and ethanol sensing. The catalyst comprises MnO_2 / MWCNTs, which is supported by a carbon ceramic electrode. This hybrid configuration leverages the extensive surface area and conductivity of MWCNTs and catalytic efficiency of MnO_2 . The resulting modified electrode demonstrated superior electrocatalytic activity toward ethanol oxidation. Furthermore, it was successfully utilized for the quantitative detection of ethanol via differential pulse voltammetry (DPV), exhibiting consistent sensitivity across a wide concentration range.

2. EXPERIMENTAL

2.1. Chemical and instrumentals

Multi-walled carbon nanotubes (MWCNTs) with a purity of 95% were sourced from Plasma Chem. GmbH (Berlin, Germany). These MWCNTs had an average outer diameter of 3–20 nm, a length of 1–10 µm, 3–15 walls, and a specific surface area of 350 m²/g. Methyltrimethoxysilane (MTMOS, 99%) and manganese (II) sulfate ($MnSO_4$) were purchased from Merck. Graphite powder (95%) was obtained from Sigma-Aldrich. All other chemicals used were of analytical grade and were procured from reputable suppliers. Electrochemical measurements were performed with a Metrohm electroanalyzer (Model 797 VA) using a standard three-electrode cell. The setup consisted of an Ag/AgCl (3.0 M KCl) reference electrode, a platinum rod counter electrode, and a modified carbon ceramic electrode (CCE) as the working electrode.

2.2. *Preparation of the carbon ceramic electrode*

The standard carbon ceramic electrode (CCE) was prepared according to a previously reported method [23]. Briefly, 0.5 mL of methyltrimethoxysilane (MTMOS) was mixed with 0.8 mL of methanol in a clean, dry test tube. Then, 0.08 mL of 11 M hydrochloric acid was added as a catalyst, and the tube was sealed with parafilm. The solution was sonicated for 5 minutes to ensure thorough mixing. Subsequently, 1.2 g of graphite powder was incorporated into the mixture, which was then sonicated for another 5 minutes to form a homogeneous paste. This paste was tightly

DOI: 10.30473/IJAC.2025.76680.1332

packed into glass tubes (5 cm in length, 3 mm inner diameter) to a depth of 5 mm. A copper wire was inserted into the paste to establish electrical contact. The electrodes were then left to dry at room temperature for 48 hours. After the drying process, the electrode surfaces were polished smooth with polishing paper and rinsed thoroughly with deionized water before use.

2.3. *Preparation of the carbon ceramic electrode*

Multi-walled carbon nanotubes (MWCNTs) were first oxidized to create surface binding sites and remove impurities, following a reported procedure [24]. Briefly, 1.0 g of MWCNTs were dispersed in 10 mL of concentrated HNO□ and the mixture was stirred for 2 hours at 35 °C and rinsed several times with double distilled water until the pH of the mixture reached 7.0. The product was filtered and oven dried at 80°C. Next, 0.09 g of the pre-treated MWCNTs was dispersed in 150 mL of deionized water using ultrasonication for 30 minutes. Potassium permanganate ($KMnO_4$, 1.58 g) was added to the suspension, which was further sonicated for 30 minutes. Afterwards, 8 mL of 3 M hydrochloric acid (HCl) was slowly added, and the mixture was stirred for approximately 30 minutes at 50 °C. The resulting suspension was transferred to a 100 mL Teflon-lined autoclave and subjected to hydrothermal treatment at 160 °C for 24 hours. Finally, the product was centrifuged, washed, and dried overnight at 70 °C to obtain highly purified MnO_2 /MWCNTs.

2.4. *Preparation of the carbon ceramic electrode*

Prior to modification, the bare carbon ceramic electrode (CCE) was polished to a mirror-like finish on polishing paper and rinsed with deionized water. A modifier suspension was prepared by dispersing 0.01 g of the MnO_2 /MWCNTs nanocomposite in 0.5 mL of tetrahydrofuran (THF) with 5 minutes of ultrasonication. Then, 10 µL of this homogeneous suspension was drop-cast onto the polished electrode surface and left to dry at room temperature. Finally, the modified electrode was rinsed thoroughly with deionized water before being employed as the working electrode in the electrochemical cell.

3. RESULTS AND DISCUSSION

3.1 Characterization of MnO_2 /MWCNTs Nanocomposite

The phase structures of the MWCNTs and the synthesized MnO_2 /MWCNTs nanocomposite were characterized by X-ray diffraction (XRD) over a 2θ range of 0° to 80° (Fig. 1). The XRD pattern of the MWCNTs (Fig. 1a) shows characteristic peaks at approximately 26° and 43°, which are typical for the graphitic structure of carbon nanotubes and align with literature values [25]. In contrast, the XRD pattern of MnO_2 /MWCNTs nanocomposite (Fig. 1b) exhibits major diffraction peaks at 2θ values of ~29°, 35.2°, 37.1°, 38.5°, 41°, 43°, 48°, 50°, 56.5°, 63°, 65°, and 69°. These peaks are indexed to the crystalline planes of α-MnO_2 , thereby confirming the successful deposition of manganese dioxide onto the MWCNT surface [26].

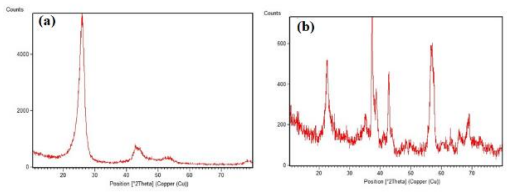

Fig. 1. Fig.1, XRD pattern of MWCNTs (a) and MnO_2 /MWCNTs nanocomposite (b)

As well, the elemental composition of MWCNTs (Fig. 2a) and MnO_2 /MWCNTs (Fig. 2b) was investigated by EDS analysis. The resulting spectrum confirms the presence of carbon, manganese and oxygen, providing definitive evidence for the successful synthesis of MnO_2 /MWCNTs nanocomposite.

DOI: 10.30473/ijac.2024.72409.1309

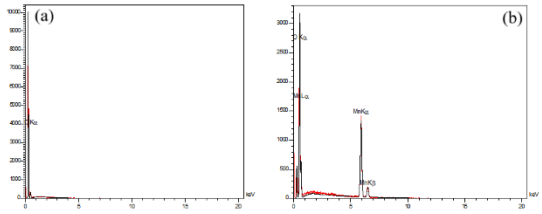

Fig.2, EDS analysis of MWCNTs (a) and MWCNTs/MnO_2 nanocomposite (b)

FE-SEM analysis was used to examine the morphology of both materials. The MWCNTs (Fig. 3a) show a uniform size distribution with an average particle size of ~94 nm. In contrast, the MnO_2 /MWCNTs nanocomposite (Fig. 3b) has a larger average particle size of ~138 nm, improved dispersion and increased thickness. These observed changes confirm the successful coating of the nanotubes with manganese dioxide.

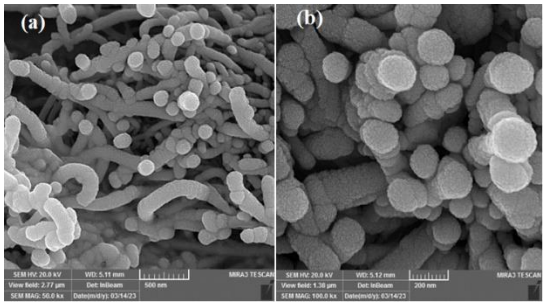

Fig.3, SEM images of MWCNTs (a) and MnO_2 /MWCNTs nanocomposite (b)

Fourier-transform infrared (FTIR) spectroscopy was used to identify the functional groups involved in stabilizing and coating the carbon nanotubes. The spectrum for MWCNTs (Fig. 4a) shows a broad band at ~3443 cm^{-1}, corresponding to O–H stretching vibrations from surface-adsorbed hydroxyl groups. The intense peak at 1577 cm^{-1} is attributed to the C=C bond stretching in the graphitic structure. Additional peaks at 1427 cm^{-1} and 1139 cm^{-1} are indicative of C–H groups and C–O–C/C–OH stretching vibrations, respectively, while the peak at 1044 cm^{-1} corresponds to C–O stretching. In contrast, the FTIR spectrum of the MnO_2 /MWCNTs nanocomposite (Fig. 4b) reveals a key new feature: a broad and intense peak at 569 cm^{-1}. This band is characteristic of Mn–O stretching and Mn–O–Mn bridge vibrations, providing direct evidence for the formation of MnO_2 and its successful deposition onto the nanotube surface.

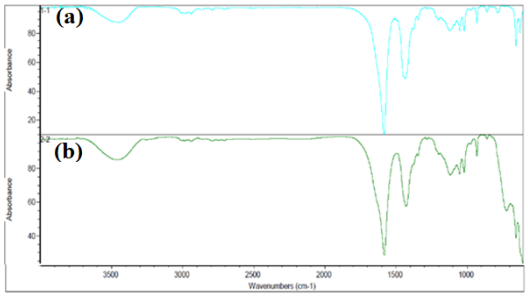

Fig. 4, FTIR spectrum of MWCNTs (a) and MnO_2 /MWCNTs nanocomposite (b)

3.2 Electrochemical characterization of MnO_2 /MWCNTs/CCE

The electrochemical properties of the CCE and the MnO_2 /MWCNTs/CCE were characterized using cyclic voltammetry. The voltammograms were recorded in a 0.1 M KCl solution containing 0.5 mM K_3 [$Fe(CN)_6$]/K_4 [$Fe(CN)_6$] (1:1 ratio). Both electrodes exhibited a well-defined, reversible redox peaks corresponding to the couple $Fe(CN)_6^{3-/4-}$ reaction (Fig. 5). A comparison of the current density responses between CCE and MnO_2 /MWCNTs/CCE revealed a marked enhancement in current density for the MnO_2 /MWCNTs/CCE. This enhancement is attributed to a substantial increase in the electroactive surface area and improved charge transfer kinetics afforded by MnO_2 /MWCNTs nanocomposite.

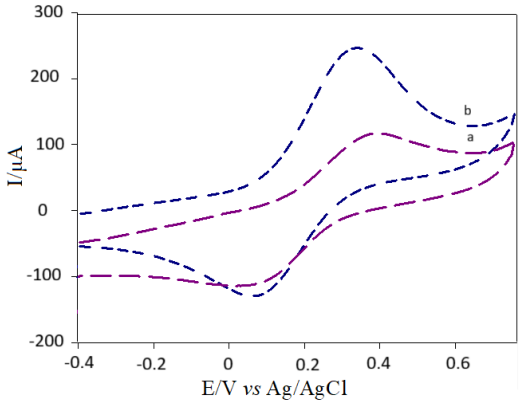

Fig.5, CV responses related to CCE (a), MnO_2 /MWCNTs/CCE (b) in a solution containing 0.1M of KCl and 500 mM of [$Fe(CN)_6$] $^{3-/4-}$ (Scan rate: 30mVs^{-1}).

The electroactive surface area (EASA) of both CCE and MnO_2 /MWCNTs/CCE was determined by cyclic voltammetry using a solution of 1.0 mM $Fe(CN)_6^{3-/4-}$ and 0.1 M KCl at different scan rates (10-100 mVs^{-1}) . The resulting peak currents

DOI: 10.30473/IJAC.2025.76680.1332

were analyzed according to the Randles-Sevcik equation (equation 1):

$$Ip = (2.69 \times 10^5).\ n^{3/2}.\ A.\ D^{1/2}.\ C.\ v^{1/2} \quad \text{Eq.1}$$

From this analysis, the EASA values were determined to be 0.151 cm² for CCE and 0.312 cm² for MnO_2 /MWCNTs/CCE, while the geometric surface area of the bare CCE was calculated about 0.08 cm^2. The markedly larger EASA of the MnO_2 /MWCNTs/CCE electrode indicates a greater density of electroactive sites. This enhancement implies that the modified CCE offers superior sensitivity and a faster response compared to the unmodified CCE.

3.3 Cyclic voltammetry studies

The electrochemical performance was evaluated by recording cyclic voltammograms of an unmodified CCE, an MWCNTs/CCE, and an MnO_2 /MWCNTs/CCE in a 0.05 M sulfuric acid solution containing 0.02 mM ethanol. Figure 6 shows the stable voltammograms obtained after several initial scans. As seen in figure 6a, the unmodified CCE showed negligible activity within the applied potential window. Modification with MWCNTs alone (Fig. 6b) resulted in a broad, weak oxidation peak around 1.1 V. In contrast, the MnO_2 /MWCNTs/CCE (Fig. 6c) exhibited a sharp and intense ethanol oxidation peak at a significantly lower potential, accompanied by a dramatically higher current density. This significant decrease in overpotential coupled with substantial increase in current density demonstrate the superior catalytic activity of the MnO_2 /MWCNTs nanocomposite toward ethanol oxidation.

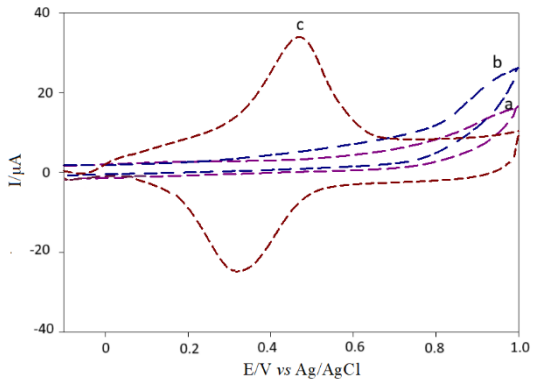

Fig.6, Comparative CVs of the unmodified CCE (a) MWCNTs/CCE (b) and the MnO_2 /MWCNTs/CCE (c) in the presence of 0.02 mM ethanol and 0.05 M sulfuric acid as supporting electrolyte, scan rate: 30 mVs^{-1}.

3.4 Ethanol electrooxidation mechanism

As observed in figure 6 (curve c), the anodic peak current for ethanol oxidation was significantly enhanced at the modified electrode compared to the unmodified electrode. Simultaneously, a substantial reduction in the oxidation overpotential was observed. According to experimental results and literature reports, the possible mechanism for ethanol oxidation on the MnO_2 /MWCNTs/CCE in acidic medium involves a combination of physical adsorption and chemisorption of ethanol molecules at the anode surface, as follows [27]:

Physical adsorption mechanism:

$$CH_3CH_2OH + MnO_2 \longrightarrow CH_3CH_2O\text{-}MnOOH$$

$$CH_3CH_2O\text{-}MnOOH \longrightarrow CH_3CHO + MnO_2 + 2H^+ + 2e$$ (acetaldehyde)

$$[CH_3CHO]_{ads} + H_2O \longrightarrow [CH_3COOH]_{ads} + 2H^+ + 2e$$ (acetic acid)

Chemisorption mechanism:

$$[C_2H_5OH]_{+3}H_2O \longrightarrow 2CO_2 + 12e + 12H^+$$

3.5 Effect of potential scan rate on ethanol oxidation

Cyclic voltammetry of a 0.02 mM ethanol solution was performed at the MnO_2 /MWCNTs/CCE across a range of scan rates from 10 to 100 mV s^{-1} (Fig. 7a). The anodic peak current increased with increasing scan rate, while the peak potential shifted positively. To investigate the reaction kinetics, the anodic peak current (Ip) was plotted against both the square root of the scan rate ($v^{1/2}$) (Fig. 7b) and the scan rate itself (v) (Fig. 7c). A strong linear relationship ($R^2 > 0.99$) was observed between Ip and $v^{1/2}$, indicating that the electrocatalytic oxidation of ethanol at this electrode is a diffusion-controlled process [28].

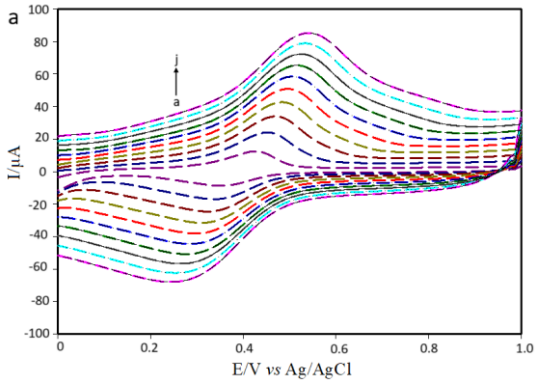

DOI: 10.30473/ijac.2024.72409.1309

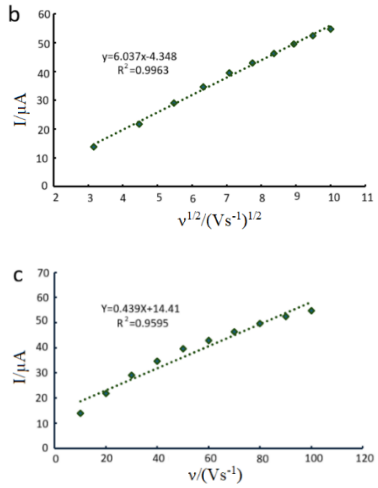

Fig.7, Cyclic voltammograms of the MnO_2 /MWCNTs/CCE at various scan rates, ranging from 10 to 100 mVs^{-1}(a→j) (a), the relationship between the (anodic) peak current and the square root of scan rate **(b)** and the relationship between the (anodic) peak current and the scan rate(c). All measurements were conducted in a 0.05 M of sulfuric acid electrolyte containing 0.02 mM ethanol.

3.6 Quantitative analysis of ethanol by MnO_2 /MWCNTs/CCE

A series of ethanol standards at varying concentrations were analyzed using differential pulse voltammetry (DPV) to generate a calibration plot. The recorded DPV responses (Fig. 8) showed anodic peaks whose current intensities were directly proportional to the ethanol concentration, as illustrated in the inset. The linear relationship observed across the 0.02 to 0.30 mM range confirms a dependable correlation between the signal and analyte concentration.

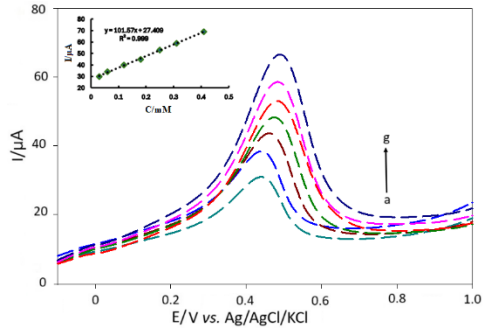

Fig.8, Differential pulse voltammograms of the MnO_2 /MWCNTs/CCE recorded in the presence of different concentrations of ethanol (0.02, 0.06, 0.10, 0.13, 0.15, 0.18, 0.21 and 0.3mM), inset: variation of the anodic peak current as a function of ethanol concentration. All of the experiments were done in a 0.05 M of sulfuric acid electrolyte solution.

3.7 Stability and repeatability Studies of MnO_2 /MWCNTs/CCE

Experimental results confirmed that the MnO_2 /MWCNTs/CCE exhibits excellent stability in the electrolyte solution, with both peak current and potential remaining nearly constant over multiple scanning cycles. After 20 consecutive cyclic voltammetry scans in 0.05 M sulfuric acid, the electrode's stability was assessed using equation 2:

Stability percentage: $=(Ip_n/Ip_1) \times 100$ Eq.2

In Equation 1, Ip_1 and Ip_n represent the first and last anodic or cathodic peak currents, respectively. The calculated stability exceeded 90% after 20 consecutive measurements, confirming the high operational stability of the MnO_2 /MWCNTs/CCE.

The limit of detection (LOD) refers to the lowest concentration of an analyte that can be reliably distinguished from the background signal. It was calculated using Equation 3:

$$\text{Limit of detection} = 3S_b/m \quad \text{Eq.3}$$

where S_b is the standard deviation of the blank response and m is the slope of the calibration curve obtained from inset of Fig. 8. To determine S_b, a blank solution consisting of 0.05 M sulfuric acid was prepared, and differential pulse voltammograms (DPVs) were recorded using the modified electrode. Seven consecutive scans were performed, and the resulting data were analyzed. The calculated detection limit for ethanol was found to be 6.2 μM, indicating high sensitivity of the MnO_2 /MWCNTs/CCE toward ethanol detection.

Repeatability is a key indicator of the method's precision and is commonly expressed as the relative standard deviation (RSD%). To assess this, a 0.04 mM ethanol solution was prepared under optimized conditions and subjected to seven consecutive measurements using the modified electrode. The resulting cyclic voltammograms were recorded, and the anodic peak currents were extracted. The RSD% was calculated using Equation 4:

$$RSD\ (\%) = (S / \bar{X}) \times 100 \quad \text{Eq. 4}$$

where S is the standard deviation and $\bar{X}$ is the mean peak current. The calculated RSD was

DOI: 10.30473/IJAC.2025.76680.1332

1.30%, indicating excellent repeatability and precision of the electrode for ethanol detection.

4. Chronoamperometric measurements

The electrode processes at the MnO_2 /MWCNTs/CCE were further probed using chronoamperometry, among other electrochemical methods. In this experiment, a constant potential of 0.5 V was applied to the working electrode while measuring the current over time for different ethanol concentrations (Fig. 9). The resulting current-time transients are characteristic of a mass transfer-limited oxidation process, consistent with the behavior predicted by the Equation 5 (Cottrell equation) [28]:

$$I = nFAD^{1/2}C^*/ \pi^{1/2}t^{1/2}$$

Eq. 5

where A, D, and C* are the real surface area (0.08 cm^2), diffusion coefficient (cm^2s^{-1}), and the bulk concentration (mol cm^{-3}), respectively. The plot of *I* versus $t^{-1/2}$ for MnO_2 /MWCNTs/CCE in the presence of ethanol shows a straight line. Based on the slope of this plot (inset of Fig. 9), the diffusion coefficient of ethanol was calculated to be 5.24×10^{-7} cm^2s^{-1}, indicating efficient mass transport at the MWCNTs/MnO_2 /CCE surface.

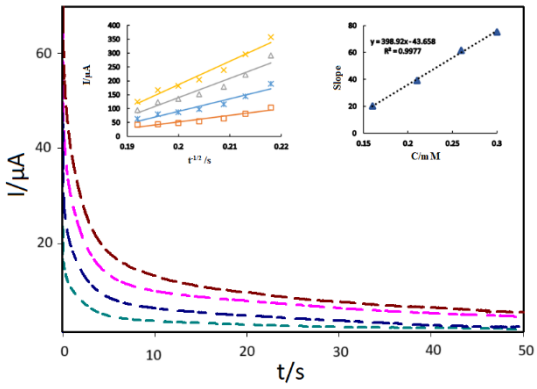

Fig.9, Chronoamperograms obtained by the MnO_2 /MWCNTs/CCE in the presence of various concentrations of ethanol (0.15, 0.20, 0.25, and 0.30 mM).

5.Conclusion

In this study, a carbon ceramic electrode (CCE) was successfully modified with a multi-walled carbon nanotube/manganese dioxide (MnO_2 /MWCNTs) nanocomposite to create a highly effective electrocatalyst. The resulting MnO_2 /MWCNTs/CCE demonstrated exceptional performance for the electrooxidation of ethanol, exhibiting a significantly lower overpotential approximately 470 mV less than the unmodified CCE which signifies markedly enhanced reaction kinetics. Furthermore, the electrode showed high sensitivity with a low detection limit of 6.2 μM for ethanol. These results confirm the composite's superior catalytic activity and its strong potential for dual applications: as an efficient anode in direct ethanol fuel cells and as a sensitive platform for electrochemical ethanol sensors.

DOI: 10.30473/ijac.2024.72409.1309

References

[1] Manochio, C., Andrade, B. R., Rodriguez, R. P., & Moraes, B. S. (2017). Ethanol from biomass: A comparative overview. *Renewable and Sustainable Energy Reviews*, *80*, 743-755. https://doi.org/10.1016/j.rser.2017.05.063

[2] Wyman, C. E. (2018). Ethanol production from lignocellulosic biomass: overview. *Handbook on Bioethanol*, 1-18.

[3] Chandel, A. K., Albarelli, J. Q., Santos, D. T., Chundawat, S. P., Puri, M., & Meireles, M. A. A. (2019). Comparative analysis of key technologies for cellulosic ethanol production from Brazilian sugarcane bagasse at a commercial scale. *Biofuels, bioproducts and biorefining*, *13*(4), 994-1014. https://doi.org/10.1002/bbb.1990

[4] Guo, Y., Liu, G., Ning, Y., Li, X., Hu, S., Zhao, J., & Qu, Y. (2022). Production of cellulosic ethanol and value-added products from corn fiber. *Bioresources and Bioprocessing*, *9*(1), 81. https://doi.org/10.1186/s40643-022-00573-9

[5] Elsaid, K., Abdelfatah, S., Elabsir, A. M. A., Hassiba, R. J., Ghouri, Z. K., & Vechot, L. (2021). Direct alcohol fuel cells: Assessment of the fuel's safety and health aspects. *International Journal of Hydrogen Energy*, *46*(59), 30658-30668. https://doi.org/10.1016/j.ijhydene.2020.12.009

[6] Matheus, C. R., & Sousa-Aguiar, E. F. (2024). Main catalytic challenges in ethanol chemistry: A review. *Catalysis Reviews*, *66*(1), 174-213. https://doi.org/10.1080/01614940.2022.2054554

[7] Altarawneh, R. M. (2021). Overview on the vital step toward addressing platinum catalyst poisoning mechanisms in acid media of direct ethanol fuel cells (DEFCs). *Energy & Fuels*, *35*(15), 11594-11612. https://doi.org/10.1021/acs.energyfuels.1c00453

[8] Reddy, L. E., Gollapudi, D., Jain, G. M., Kolluru, S., & Ramesh, G. V. (2023). Recent progress in the development of Platinum-based electrocatalysts for the oxidation of ethanol in fuel cells. *Materials Today: Proceedings*, *92*, 636-641. https://doi.org/10.1016/j.matpr.2023.04.135

[9] Alothman, Z. A., Bukhari, N., Wabaidur, S. M., & Haider, S. (2010). Simultaneous electrochemical determination of dopamine and acetaminophen using multiwall carbon nanotubes modified glassy carbon electrode. *Sensors and Actuators B: Chemical*, *146*(1), 314-320. https://doi.org/10.1016/j.snb.2010.02.024

[10] Wu, F. H., Zhao, G. C., & Wei, X. W. (2002). Electrocatalytic oxidation of nitric oxide at multi-walled carbon nanotubes modified electrode. *Electrochemistry Communications*, *4*(9), 690-694. https://doi.org/10.1016/S1388-2481(02)00435-6

[11] Zhao, G. C., Zhang, L., Wei, X. W., & Yang, Z. S. (2003). Myoglobin on multi-walled carbon nanotubes modified electrode: direct electrochemistry and electrocatalysis. *Electrochemistry Communications*, *5*(9), 825-829. https://doi.org/10.1016/j.elecom.2003.07.006

[12] Saboor, F. H., & Ataei, A. (2024). Decoration of metal nanoparticles and metal oxide nanoparticles on carbon nanotubes. *Advanced Journal of Chemistry, Section A*, *7*(2), 122-145. DOI: 10.48309/ajca.2024.416693.1420

[13] Yang, S. Y., Vecitis, C. D., & Park, H. (2019). Electrocatalytic water treatment using carbon nanotube filters modified with metal oxides. *Environmental Science and Pollution Research*, *26*(2), 1036-1043. https://doi.org/10.1007/s11356-017-8495-6

[14] Jiang, L. C., & Zhang, W. D. (2010). A highly sensitive nonenzymatic glucose sensor based on CuO nanoparticles-modified carbon nanotube electrode. *Biosensors and Bioelectronics*, *25*(6), 1402-1407. https://doi.org/10.1016/j.bios.2009.10.038

[15] Fang, B., Zhang, C., Zhang, W., & Wang, G. (2009). A novel hydrazine electrochemical sensor based on a carbon nanotube-wired ZnO nanoflower-modified electrode. *Electrochimica Acta*, *55*(1), 178-182. https://doi.org/10.1016/j.electacta.2009.08.036

[16] Liu, Z., Wang, J., Xie, D., & Chen, G. (2008). Polyaniline- coated Fe_3O_4 nanoparticle–carbon-nanotube composite and its application in electrochemical biosensing. *Small*, *4*(4), 462-466. https://doi.org/10.1002/smll.200701018

[17] Wang, Y., Hu, G., Zheng, D., Dong, J., & Wang, J. (2023). High-capacitance manganese dioxide oxide/carbon nanotube/carbon felt as a bioanode for enhanced energy output in microbial fuel cells. *Coatings*, *13*(6), 1043. https://doi.org/10.3390/coatings13061043

[18] Amade, R., Vila-Costa, M., Hussain, S., Casamayor, E. O., & Bertran, E. (2015). Vertically aligned carbon nanotubes coated with manganese dioxide as cathode material for microbial fuel cells. *Journal of Materials Science*, *50*(3), 1214-1220. https://doi.org/10.1007/s10853-014-8677-2

[19] Xu, W., Xue, S., Yi, H., Jing, P., Chai, Y., & Yuan, R. (2015). A sensitive electrochemical aptasensor based on the co-catalysis of hemin/G-quadruplex, platinum nanoparticles and flower-like MnO_2 nanosphere functionalized multi-walled carbon nanotubes. *Chemical Communications*, *51*(8), 1472-1474. https://doi.org/10.1039/C4CC08860C

[20] Hameed, R. A., Fetohi, A. E., Amin, R. S., & El-Khatib, K. M. (2015). Promotion effect of manganese oxide on the electrocatalytic activity of Pt/C for methanol oxidation in acid

medium. *Applied Surface Science*, *359*, 651-663. https://doi.org/10.1016/j.apsusc.2015.10.130
[21] Panrod, C., Themsirimongkon, S., Waenkaew, P., Inceesungvorn, B., Juntrapirom, S., & Saipanya, S. (2018). Effect of noble metal species and compositions on manganese dioxide-modified carbon nanotubes for enhancement of alcohol oxidation. *International Journal of Hydrogen Energy*, *43*(35), 16866-16880. https://doi.org/10.1016/j.ijhydene.2017.12.145
[22] Nouralishahi, A., Khodadadi, A. A., Mortazavi, Y., Rashidi, A., & Choolaei, M. (2014). Enhanced methanol electro-oxidation activity of Pt/MWCNTs electro-catalyst using manganese oxide deposited on MWCNTs. *Electrochimica Acta*, *147*, 192-200. https://doi.org/10.1016/j.electacta.2014.09.113
[23] Tsionsky, M., Gun, G., Glezer, V., & Lev, O. (1994). Sol-gel-derived ceramic-carbon composite electrodes: introduction and scope of applications. *Analytical Chemistry*, *66*(10), 1747-1753. https://doi.org/10.1021/ac00082a024
[24] Tan, X., Li, M., Cai, P., Luo, L., & Zou, X. (2005). An amperometric cholesterol biosensor based on multiwalled carbon nanotubes and organically modified sol-gel/chitosan hybrid composite film. *Analytical Biochemistry*, *337*(1), 111-120. https://doi.org/10.1016/j.ab.2004.10.040
[25] Wang, X., Chu, J., Yan, H. J., & Zhang, H. K. (2022). Synthesis and characterization of MnO_2/Eggplant carbon composite for enhanced supercapacitors. *Heliyon*, *8*(9). https://doi.org/10.1016/j.heliyon.2022.e10631
[26] Boamah, R., Agyei-Tuffour, B., Dodoo-Arhin, D., Nyankson, E., Brobbey, K. J., Obada, D., & Mohammed, L. (2023). Activated cashew carbon-manganese oxide based electrodes for supercapacitor applications. *Scientific African*, *20*, e01647. https://doi.org/10.1016/j.sciaf.2023.e01647
[27] Li, Y., Wei, X., Han, S., Chen, L., & Shi, J. (2021). MnO_2 electrocatalysts coordinating alcohol oxidation for ultra- durable hydrogen and chemical productions in acidic solutions. *Angewandte Chemie*, *133*(39), 21634-21642. **https://doi.org/10.1002/ange.202107510**
[28] Bard, A. J., Faulkner, L. R., & White, H. S. (2022). *Electrochemical methods: fundamentals and applications*. John Wiley & Sons.

DOI: 10.30473/ijac.2024.72409.1309

MnO_2 /MWCNTs Nanocomposite Modified Carbon Ceramic Electrode: A Renewable Platform for Ethanol Oxidation

Tahereh Rohani*[1], Sayed Zia Mohammadi[1], Masood Nayebli[1]

[1]Department of Chemistry, Payame Noor University, 19395-4697, Tehran, Iran

e-mail: Rohani@pnu.ac.ir

Received: 2 October 2024 **Accepted:** 22 October 2024
DOI: 10.30473/ijac.2024.72409.1309
Received: 2 October 2024 **Accepted:** 22 October 2024
DOI: 10.30473/ijac.2024.72409.1309

چکیده

در کار حاضر، الکترود سرامیک کربنی تهیه شده و با نانوکامپوزیت دی‌اکسید منگنز/نانولوله‌های کربنی چند دیواره (MnO_2 /MWCNTs)اصلاح شد. نانولوله‌های کربنی چنددیواره با دی‌اکسید منگنز ترکیب گردید تا خواص کاتالیستی آن‌ها بهبود یابد. نانوکامپوزیت حاصل برای بررسی کارایی در کاتالیز اکسیداسیون اتانول مورد ارزیابی قرار گرفت. مشخصه‌یابی کاتالیست با استفاده از پراش پرتو ایکس (XRD) ، میکروسکوپ الکترونی روبشی(SEM) و طیف‌سنجی مادون قرمز تبدیل فوریه (FT-IR) انجام شد. خواص الکتروشیمیایی از طریق ولتامتری چرخه‌ای(CV) ، ولتامتری پالسی تفاضلی (DPV) و کرونوآمپرومتری بررسی گردید. نتایج بدست آمده، محدوده‌ی خطی ۰/۰۲ تا ۰/۳ میلی‌مولار، حد تشخیص ٦/٢ میکرومولار و ضریب نفوذ $5/24 \times 10^{-7}$ cm^2s^{-1} برای اتانول را نشان داد. سطح ویژه و رسانایی بالای نانولوله‌های کربنی چنددیواره، در ترکیب با فعالیت کاتالیستی MnO_2، پتانسیل نانوکامپوزیت تهیه‌شده را برای کاربرد در پیل‌های سوختی با کارایی بالا به نمایش می‌گذارد.

کلید واژه ها

اکسیداسیون اتانول، پیل سوختی، MnO_2، نانولوله‌های کربنی چنددیواره